



Particle-scale origins of shear strength in granular media

Farhang Radjai

► To cite this version:

Farhang Radjai. Particle-scale origins of shear strength in granular media. Second Euro- Mediterranean Symposium on Advances in Geomaterials and Structures, May 2008, Tunisia. hal-00223914

HAL Id: hal-00223914

<https://hal.science/hal-00223914>

Submitted on 29 Jan 2008

HAL is a multi-disciplinary open access archive for the deposit and dissemination of scientific research documents, whether they are published or not. The documents may come from teaching and research institutions in France or abroad, or from public or private research centers.

L'archive ouverte pluridisciplinaire **HAL**, est destinée au dépôt et à la diffusion de documents scientifiques de niveau recherche, publiés ou non, émanant des établissements d'enseignement et de recherche français ou étrangers, des laboratoires publics ou privés.

Particle-scale origins of shear strength in granular media

Farhang Radjai

LMGC, CNRS-Université Montpellier 2, CC048, 34095 Montpellier, France.
radjai@lmgc.univ-montp2.fr.

Abstract. The shear strength of cohesionless granular materials is generally attributed to the compactness or anisotropy of their microstructure. An open issue is how such compact or anisotropic microstructures, and thus the shear strength, depend on the particle properties. We first recall the role of fabric and force anisotropies with respect to the critical-state shear stress. Then, a model of accessible geometrical states in terms of particle connectivity and contact anisotropy is presented. This model incorporates in a simple way the fact that, due to steric exclusions, the highest levels of connectivity and anisotropy cannot be reached simultaneously, a property that affects seriously the shear strength. We also analyze the force anisotropy in the light of the specific role of weak forces in sustaining strong force chains and thus the main mechanism that underlies anisotropic force patterns. Finally, we briefly discuss the effect of interparticle friction, particle shape, size polydispersity and adhesion.

keyword: granular media; shear strength; fabric anisotropy; weak and strong forces.

1 Introduction

Since the early work of Coulomb in 1773, the plastic yield behavior of granular materials has remained an active research field in close connection with soil mechanics and powder technology [Mitchell and Soga(2005), Nedderman(1992)]. According to the Mohr-Coulomb yield criterion, for normal and shear stresses σ and τ acting on a slip plane, the plastic threshold τ_c is the sum of two terms:

$$\tau_c = c + \sigma \tan \varphi, \quad (1)$$

where c is a cohesive strength and φ is the internal angle of friction depending only on the nature of the granular material. This criterion expresses the pressure dependence of shear strength which is a distinctive feature of granular media. Given (1), the shear strength of cohesionless materials ($c = 0$) can be represented by the (dimensionless) stress ratio $\tau_c/\sigma = \mu_c = \tan \varphi$. Since the angle φ is a bulk property, it can be expressed in terms of stress invariants. Let σ_α ($\alpha = 1, 2, 3$) be stress principal values. The average stress is $p = (\sigma_1 + \sigma_2)/2$ in 2D and $p = (\sigma_1 + \sigma_2 + \sigma_3)/3$ in 3D. We define the stress

deviator by $q = (\sigma_1 - \sigma_2)/2$ in 2D and $q = (\sigma_1 - \sigma_3)/3$ in 3D under axisymmetric conditions ($\sigma_2 = \sigma_3$). With these notations, it can be shown that $\sin \varphi = q/p$ in 2D and $\sin \varphi = 3q/(2p + q)$ in 3D.

This picture of shear strength in granular media holds as a basic fact although the complex plastic behavior of granular media can not be reduced to a single strength parameter. In particular, the shear strength and plastic flow (dilatancy) depend on the granular structure and direction of loading, the latter reflecting the anisotropy of the structure. Since the shear strength is state-dependent, it cannot be considered as a material property unless attributed to a well-defined granular state. The internal angle of friction φ is often associated with the critical state (steady state or residual state) reached after long monotonous shearing; see Fig. 1. This state is characterized by a solid fraction ρ_c independent of the loading history and initial conditions [Wood(1990)].

The critical-state strength is below the peak shear stresses occurring for dense states with solid fraction $\rho_0 > \rho_c$, but these states are metastable and often lead to strain localization [Darve and Laouafa(2000), Vardoulakis and Sulem(1995)]. For loose states with $\rho_0 < \rho_c$, the critical state is reached asymptotically following diffuse rearrangements. Hence, apart from these transients, which are governed by the evolution of internal variables pertaining to the microstructure and are important in formulating elasto-plastic models, the critical-state shear strength represents a stable plastic threshold for a granular material. In this paper, we are interested in the critical-state strength as a material property of cohesionless granular materials. The critical-state friction angle φ_c can be described as a coarse-grained (or homogenized) friction angle between two granular layers sliding past each other. Nevertheless, the macroscopic status of φ_c as a Coulomb friction angle, on the same grounds as those of dry friction between solid bodies, should not eclipse the

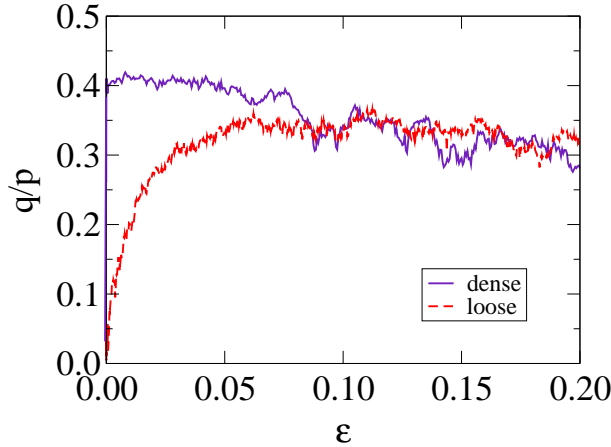


Figure 1: Normalized shear stress as a function of cumulative shear strain in a 2D simple shear simulation by the contact dynamics method for two different values of the initial solid fraction.

fact that the granular friction angle is a bulk property to which adequate tensorial stress analysis should be applied (this was indeed the contribution of Mohr) and where the slip planes are not *a priori* defined, in contrast to solid friction which is a surface property at the macroscopic scale [Radjai et al.(2004)]. Depending on the boundary conditions, the critical state occurs either homogeneously in the whole volume of a granular sample or inside a thick layer of several particle diameters in the advent of strain localization [Bardet and Proubet(1992), Herrmann et al.(1995), Vermeer(1990), Moreau(1997)]. In both configurations, φ_c stems from various granular phenomena such as friction between particles, anisotropy of the microstructure, organization of force networks and dissipation due to inelastic collisions. We consider below these effects and their respective roles in enhancing or restraining granular friction.

2 Effect of interparticle friction

While solid friction between particles underlies the frictional behavior of granular materials, it is not obvious how and through which physical mechanisms it comes into play. If shear deformation took place as a result of sliding between all contacts along a slip plane, the friction angle φ_c would simply echo the friction between particles. An example of such a configuration is a regular pile of cubic blocs subjected to a vertical load. Horizontal shearing of this pile implies sliding between at least two rows so that the shear strength of the pile is a straightforward effect of friction between the blocs. However, discrete numerical simulations suggest that in sheared granular materials, rolling prevails over sliding [Radjai et al.(1998)]. In quasistatic shear, sliding occurs at only $\simeq 10\%$ of contacts, and these sliding contacts belong essentially to weak contacts (see below) oriented on average along the minor principal stress directions [Radjai et al.(1999), Staron and Radjai(2005), Staron et al.(2005)]. Hence, the relationship between φ_c and the local friction angle φ_s involves the inhomogeneous distribution of forces and mobilization (or activation) of the friction force at rolling contacts.

This relationship is far from linear as shown in Fig. 2. The critical-state coefficient $\mu_c = \tan \varphi_c$ is above $\mu_s = \tan \varphi_s$ at small values of the latter, and at larger values it tends to a plateau $\mu_\infty < \mu_s$ [Corriveau et al.(1997), Taboada et al.(2006)]. The transition from $\mu_c - \mu_s < 0$ to $\mu_c - \mu_s > 0$ occurs at $\mu_c = \mu_s \simeq 0.5$. Beyond $\mu_s = 0.5$, μ_c is practically independent of μ_s . The independence of φ_c with respect to φ_s at large values of the latter indicates that the role of interparticle friction is more subtle than expected from simple models. Moreover, the nonzero value of φ_0 shows clearly that the interparticle friction is not the only source of frictional behavior in the critical state [Roux and Radjai(2001)]. The *direct* contribution of interparticle friction to shear strength, i.e. without interposition by the microstructure as will be analyzed below, may be evaluated from a decomposition of the shear stress. The stress tensor $\sigma_{\alpha\beta}$ in a control volume V can be expressed as [Rothenburg and Selvadurai(1981), Christoffersen et al.(1981), Moreau(1997), Bagi(1999), Staron et al.(2005)]

$$\sigma_{\alpha\beta} = n_b \langle \ell_\alpha^i f_\beta^i \rangle, \quad (2)$$

where n_b is the number density of bonds (contacts), ℓ_α^i is the α -component of the branch vector ℓ^i joining the centers of particles at contact i and f_β^i is the β -component of the force vector \mathbf{f} acting at the contact i between the two particles.

The contribution of friction forces can be estimated by replacing in equation (2) \mathbf{f} by $\mathbf{f} \cdot \mathbf{t} \mathbf{t}$, where \mathbf{t} is the unit vector along the friction force. The contribution of normal forces is the complementary tensor obtained by replacing \mathbf{f} by $\mathbf{f} \cdot \mathbf{n} \mathbf{n}$, where \mathbf{n} is the unit vector perpendicular to the contact plane. The corresponding shear strengths q_t and q_n can then be calculated in the critical state. Numerical simulations show that the ratio q_t/q is quite low (below 10%)[Cambou(1993)]. This counterintuitive finding underlines the role of interparticle friction as a parameter acting “behind the scenes” rather than a direct actor of shear strength. Our simulations show that, due to disorder and force/moment balance conditions as well as kinematic constraints such as rotation frustration, the friction forces inside a granular packing are strongly coupled with normal forces. For example, highly mobilized friction forces are rare events and the distribution of friction forces reflects for the most part that of normal forces. We consider below such effects in connection with granular microstructure.

3 Harmonic representation of the microstructure

The microscopic expression of the stress tensor in equation (2) is an arithmetic mean involving the branch vectors and contact forces. Hence, for analyzing the particle-scale origins of the shear strength, we need a statistical description of the granular microstructure and force transmission. Noticing that the shear stress corresponds to the deviation

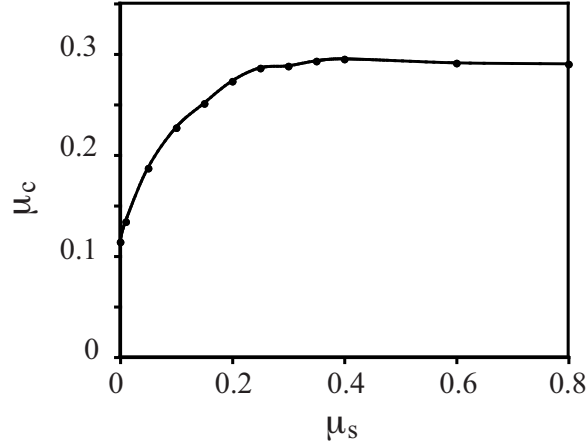


Figure 2: The critical-state friction coefficient μ_c as a function of sliding friction coefficient μ_s between particles in biaxial shearing of a sample of 5000 particles.

of stress components from the mean stress $p = \text{tr}(\boldsymbol{\sigma})/d$ (for space dimension d) along different space directions, the useful information for this analysis is the density and average force of all contacts pointing in the same direction as a function of this direction. These functions can be expanded in Fourier series in 2D and in spherical harmonics in 3D [Rothenburg and Bathurst(1989), Ouadfel and Rothenburg(2001)]. Since the contacts have no polarity, the period is π .

For illustration, we consider here only the 2D expansions truncated beyond the second term:

$$\begin{cases} P_\theta(\theta) &= \frac{1}{\pi} \{1 + a \cos 2(\theta - \theta_b)\}, \\ \langle f_n \rangle(\theta) &= \langle f \rangle \{1 + a_n \cos 2(\theta - \theta_n)\}, \\ \langle f_t \rangle(\theta) &= \langle f \rangle a_t \sin 2(\theta - \theta_t), \end{cases} \quad (3)$$

where P_θ is the probability density function of contact normals, and f_n and f_t are the force components along (radial) and perpendicular to (orthoradial) the branch vector, respectively. The parameters a , a_n and a_t are the anisotropies of branch vectors, radial forces and orthoradial forces, respectively, θ_b , θ_n and θ_t being the corresponding privileged directions. The sine function for the expansion of the orthoradial component f_t is imposed by the requirement that the mean orthoradial force is zero to satisfy the balance of force moments over particles whereas the mean radial force $\langle f \rangle$ is positive (repulsive). We also note that for circular and spherical particles the radial and orthoradial force components coincide with normal and tangential forces, respectively.

This *harmonic representation* with only three anisotropy parameters provides a good approximation for numerical data. Using the functions (3), the stress components $\sigma_{\alpha\beta}$ can be written as an integral over space directions:

$$\sigma_{\alpha\beta} = n_b \langle \ell \rangle \int_0^\pi \{ \langle f_n \rangle(\theta) n_\alpha(\theta) + \langle f_t \rangle(\theta) t_\beta(\theta) \} P_\theta(\theta) d\theta, \quad (4)$$

where $n_x = \cos(\theta)$ and $n_y = \sin(\theta)$, $t_x = -\sin(\theta)$ and $t_y = \cos(\theta)$. It has been also assumed that the branch vector lengths ℓ are not correlated with forces.

Equation (4) together with the harmonic approximation expressed in equation (3) yield the following expression for the normalized stress deviator [Radjai et al.(2004)]:

$$\frac{q}{p} \simeq \frac{1}{2} \{ a \cos 2(\theta_\sigma - \theta_b) + a_n \cos 2(\theta_\sigma - \theta_n) + a_t \cos 2(\theta_\sigma - \theta_t) \}, \quad (5)$$

where θ_σ is the major principal direction of the stress tensor. In deriving equation (5), the cross products among the anisotropies have been neglected. In the critical state, the privileged directions coincide, i.e. $\theta_b \simeq \theta_n \simeq \theta_t \simeq \theta_\sigma$, so that [Rothenburg and Bathurst(1989), Ouadfel and Rothenburg(2001)]

$$\frac{q_c}{p} \simeq \frac{1}{2} \{ a_c + a_{nc} + a_{tc} \}, \quad (6)$$

where the anisotropy parameters refer to the critical state. In 3D, a similar relation can be established by means of spherical harmonics [Azéma et al.(2008)]:

$$\frac{q_c}{p} \simeq \frac{2}{5} \{ a_c + a_{nc} + a_{tc} \} \quad (7)$$

These relations exhibit two microscopic sources of the shear strength in a granular packing: 1) fabric anisotropy, represented by the parameter a and 2) force anisotropy, captured into the parameters a_n and a_t . Hence, the material parameters influence the shear strength via fabric and force anisotropies. For example, the saturation of φ_c for $\varphi_s > 0.5$ (section 2) means that, increasing the interparticle friction beyond this limit does not enhance anisotropy.

4 Accessible geometrical states

In this section, we focus on the fabric anisotropy a which represents the excess and loss of contacts along different space directions with respect to the average contact density. The latter is commonly represented by the coordination number z (mean number of contacts per particle). In a granular material, z is bounded between two limits z_{min} and z_{max} . The lower bound z_{min} is dictated by the force balance requirement. For example, stable particles often involve more than three contacts in 2D and more than four contacts in 3D. On the other hand, the upper bound z_{max} is constrained by steric exclusions [Troade et al.(2002)]. For example, in 2D for a system of monodisperse particles, a particle can not have more than 6 contacts. In practice, this limit is reduced to 4 as a result of disorder.

Within the harmonic approximation, the geometrical state of a granular system is defined by its position in the space of coordinates (z, a) . We define two limit states: 1) the loosest isotropic state, characterized by $(z = z_{min}, a = 0)$, and 2) the densest isotropic state, characterized by $(z = z_{max}, a = 0)$. These states can be reached only by complex loading. For example, it is generally difficult to bring a granular system towards a dense isotropic state via isotropic compaction. The reason is that the rearrangements occur mainly in the presence of shearing, and the latter leads to fabric anisotropy.

It is natural to assume that all accessible geometrical states are enclosed between the two isotropic limit states. In order to represent the geometrical states, it is useful to define the *state function*

$$E(\theta) = zP_\theta(\theta) = \frac{z}{\pi} \{1 + a \cos 2(\theta - \theta_b)\}. \quad (8)$$

The two limit isotropic states are $E_{min} = z_{min}/\pi$ and $E_{max} = z_{max}/\pi$. The assumption that the geometrical states are constrained to stay between the two isotropic limit states, implies that the anisotropy a can not exceed a maximum a_{max} depending on the value of z . With harmonic approximation (8), we obtain

$$a_{max}(z) = \min \left\{ 2 \left(1 - \frac{z_{min}}{z} \right), 2 \left(\frac{z_{max}}{z} - 1 \right) \right\}. \quad (9)$$

This function is shown in Fig. 3. By construction, $a_{max}(z_{min}) = a_{max}(z_{max}) = 0$. The largest anisotropy is

$$a_c = a_{max}(z_c) = 2 \frac{a_{max} - a_{min}}{a_{max} + a_{min}}, \quad (10)$$

with $z_c = (z_{min} + z_{max})/2$. According to equation (10), a_{max} increases with z for $z < z_c$, and it declines with z for $z > z_c$. When $a = a_c$ is reached along a monotonic path,

neither anisotropy nor coordination number evolve since both contact gain and contact loss are saturated. In this picture, the critical state corresponds to the intersection between the two regimes with $z = z_c$ and $a = a_c$. In 2D with weakly polydisperse circular particles and $\mu_s > 0.5$, a good fit is provided by assuming $z_{min} = 3$ and $z_{max} = 4$. This yields $z_c = 3.5$ and $a_c = 2/7$. For lower values of μ_s , a_c declines.

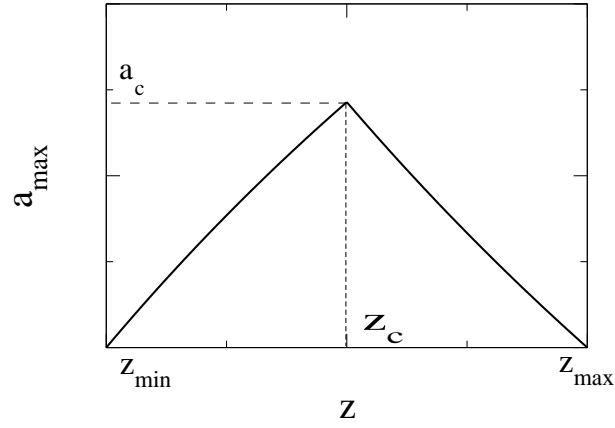


Figure 3: Domain of accessible geometrical states based on the harmonic representation of granular microstructure.

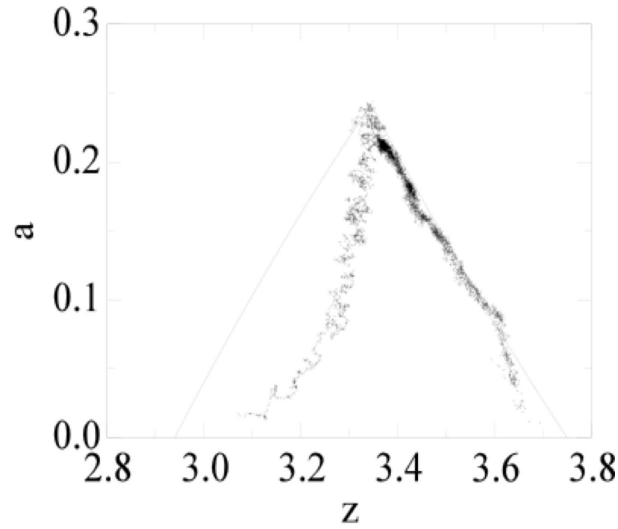


Figure 4: Evolution of the geometrical state of a sheared packing for two different initial states simulated by the contact dynamics method.

Fig. 4 shows the evolution of a with z in simulated biaxial compression of two initially isotropic samples with initial coordination numbers $z_0 = 3.1$ and $z_0 = 3.7$. In both simulations, z tends to the same critical-state value $z_c \simeq 3.35$ with $a_c \simeq 0.24$. Remarkably, the anisotropy of the dense packing reaches and then follows closely the limit states. Equation (9) provides here an excellent fit to the data with only one fitting parameter z_{max} . In the loose case, the trajectory remains entirely inside the domain of accessible states and the limit states are reached only at the critical state

Equation (10) predicts that the critical state anisotropy a_c increases with $z_{max} - z_{min}$. The shape, size and frictional characteristics of the particles may therefore influence a_c via z_{min} and z_{max} . For example, increasing the sliding friction between the particles allows for lower values of z_{min} (stable configurations with less contacts) without changing z_{max} (which depends only on steric exclusions) and leads to larger values of a_c .

One interesting aspect of the model of accessible states presented in this section is to show that the largest values of a and z can not be reached simultaneously. The critical value a_c is not obtained with z_{max} but with z_c which is below z_{max} . But higher levels of force anisotropies a_{nc} and a_{tc} can be achieved with higher values of z .

5 Weak and strong force networks

According to equation (10), the shear strength is proportional to force anisotropies a_{nc} and a_{tc} in the critical state. As for fabric anisotropy a , which was discussed in the last section, we would like to analyze here the mechanisms that underly force anisotropies. A basic feature of force distribution in granular media is the occurrence of numerous weak forces together with a subnetwork of strong forces appearing often sequentially (force

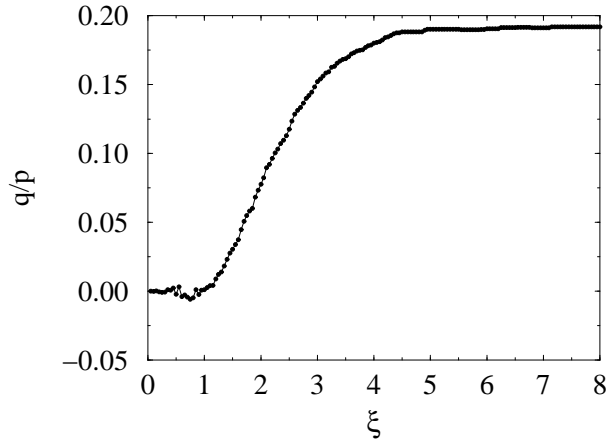


Figure 5: The partial shear stress, normalized by the mean stress, as a function of force threshold ξ .

chains). The probability density function (pdf) $P_n(f_n)$ of normal forces in a macroscopically homogeneous system in the critical state is such that more than 58% of contact forces are below the mean force $\langle f_n \rangle$ and they have a nearly uniform distribution [Radjai et al.(1996), Mueth et al.(1998), Tsoungui et al.(1998)]. These *weak* forces contribute only $\simeq 29\%$ to the mean stress p . The pdf of *strong* forces (above the mean normal force $\langle f_n \rangle$) decays exponentially [Radjai1996a, Coppersmith1996a, Radjai1999, Majumdar2005, Metzger2004]. The very large number of weak forces, reflecting the arching effect, is a source of weakness for the system. Weak regions inside a packing correspond to locally weak pressures and they are more susceptible to fail. A quantitative analysis of grain rearrangements indicates that during a quasistatic evolution those weak regions undergo local rearrangements, and nearly all sliding contacts are localized in weak regions [Staron et al.(2002), Staron et al.(2005), Nicot and Darve(2006)].

Let $\mathcal{S}(\xi)$ be the set of contacts with a normal force $f_n < \xi \langle f_n \rangle$. The set $\mathcal{S}(\infty)$ is the whole contact set. The weak and strong sets are $\mathcal{S}(1)$ and $\mathcal{S}(\infty) - \mathcal{S}(1)$, respectively. The partial shear stress $q(\xi)/p$ and the fabric and force anisotropies $a(\xi)$, $a_n(\xi)$ and $a_t(\xi)$ can be calculated as a function of ξ [Radjai et al.(1998)]. Our simulations show that $q(\xi) \simeq 0$; see Fig. 5. This means that nearly the whole stress deviator is carried by the strong contact network, the weak contacts contributing only to the mean stress. Hence, the total stress tensor $\boldsymbol{\sigma}$ is a sum of two terms:

$$\boldsymbol{\sigma} = p_w \mathbf{I} + \boldsymbol{\sigma}_s, \quad (11)$$

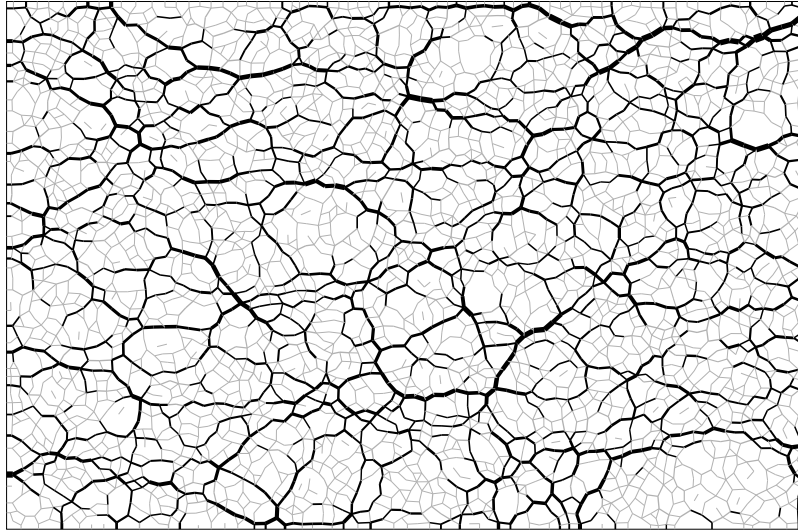


Figure 6: Weak and strong normal forces represented in two different grey levels. Line thickness is proportional to the normal force.

where \mathbf{I} is the unit tensor, p_w is the weak pressure, and σ_s represents the strong stress tensor. Hence, from the stress transmission viewpoint, the weak contact set is a “liquidlike” phase whereas the strong contact set appears as a “solidlike” backbone transmitting shear stresses. The weak and strong networks are shown in Fig. 6 in thickness of segments joining particle centers for an assembly of 4000 particles subjected to biaxial compression. The zero shear stress in the weak network implies that, according to equation (6), at least one of the corresponding anisotropies is negative. Since the critical-state angles are assumed to be equal ($\theta_b \simeq \theta_n \simeq \theta_t \simeq \theta_\sigma$), a negative value corresponds to a rotation $\pi/2$ of the principal axes. Indeed, our numerical data show that the privileged direction of weak contacts is perpendicular to the major principal stress direction [Radjai et al.(1998)]. The strong forces occur at contacts that are, on average, aligned with the major principal direction of the stress tensor. Lateral weak forces prop the particles against deviations from alignment at strong contacts. In other words, the weak contacts play the same stabilizing role with respect to the particles sustaining strong forces as the counterforts with respect to an architectural arch. This *bimodal* transmission of shear stresses corresponds thus to a statistical description of arching effect in granular media.

This stress-fabric correlation can be interpreted as a way for a granular system to optimize the shear strength. Indeed, the stress deviator q increases if a larger number of strong forces occur at contacts aligned with the major principal direction, implying thus a surplus of weak contacts in the perpendicular direction. This *weakening* of forces at contacts pointing in one direction has the same effect for force anisotropy as the loss of contacts in the same direction for fabric anisotropy. As a result, force weakening in the weak network is all the more efficient as it leads to lower amount of contact loss. This condition can, for example, be achieved for higher level of connectivity, i.e. larger values of z in the critical state.

6 Effect of material parameters

In this section, we briefly discuss the effect of several material parameters with respect to the mechanisms that underly shear strength in granular media. More details will be given elsewhere.

There are several shape parameters that may lead to enhanced shear strength through force anisotropy or fabric anisotropy. We consider here polygonal particles as compared to circular particles [Azéma et al.(2007)]. The first sample, denoted S1, is composed of 14400 regular pentagons of three different diameters: 50% of diameter 2.5 cm, 34% of diameter 3.75 cm and 16% of diameter 5 cm. The second sample, denoted S2, is composed of 10000 disks with the same polydispersity. The coefficient of friction is 0.4 between particles and 0 with the walls. At equilibrium, both numerical samples are in isotropic stress state. The solid fraction is 0.80 for S1 and 0.82 for S2. The isotropic samples are subjected to vertical compression by downward displacement of the top wall. Figure 7 displays the evolution of a as a function of the cumulative shear strain ε_q in both packings. In both cases, a increases from 0 to its largest value in the critical state. Surprisingly, the fabric anisotropy is quite weak in the pentagon packing whereas the

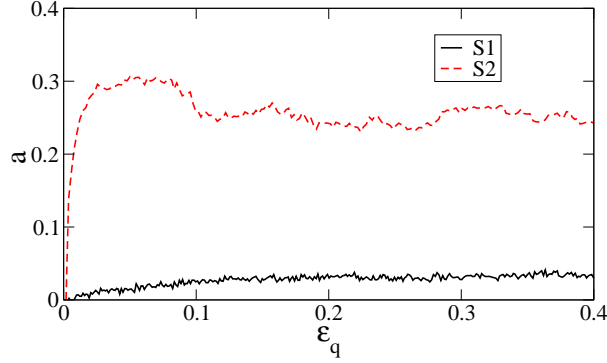


Figure 7: Evolution of the anisotropy a with cumulative shear strain ε_q for a packing of pentagons (S1) and a packing of disks (S2).

disk packing is marked by a much larger anisotropy ($\simeq 0.3$). Fig. 8 shows the evolution of a_n and a_t . We see that, in contrast to fabric anisotropies, the force anisotropies in the pentagon packing are always above those in the disk packing. This means that the aptitude of the pentagon packing to develop large force anisotropy and strong force chains is more dependent on particle shape than on the buildup of an anisotropic structure.

According to equation (6), in spite of the weak fabric anisotropy a , the larger force anisotropies a_n and a_t allow the pentagon packing to achieve higher levels of shear strength compared to the disk packing, as shown in Fig. 9. Our numerical data show that the strong force anisotropy of the polygon packing results from the edge-to-edge contacts that capture most strong force chains, whereas vertex-to-edge contacts belong mostly to the weak network. The pentagons provide thus an interesting example where the role of fabric anisotropy in shear strength is marginal. Similar conclusions hold for polyhedral particles in 3D [Azéma et al.(2008)].

The effect of the coefficient of friction μ_s between particles on the shear strength was discussed in section 2. The saturation of the critical-state friction angle φ_c with increasing μ_s is related to the fact that, due to disorder, particle equilibria are fundamentally controlled by normal forces. Ideal situations where friction needs to be fully mobilized over a large number of contacts exist but are marginal. For example, a column of particles each with two contacts may in principal exist, but is of practically zero chance to occur within a disordered granular material. The effect of μ_s over a_c manifests itself through z_{min} which decreases with μ_s . On the other hand, larger values of μ_s allow for reinforced stabilizing effect of weak contacts, increasing thereby force anisotropies and thus shear strength.

The effect of adhesion is to allow for tensile forces mainly in the direction of extension between the particles. We find that the tensile forces between particles play the same stabilizing role with respect to the strong compressive forces as the weak network [Radjai et al.(2001)]. Remark that the privileged direction of weak compressive forces coincides with that of tensile forces. As a result, the main contribution to the shear strength

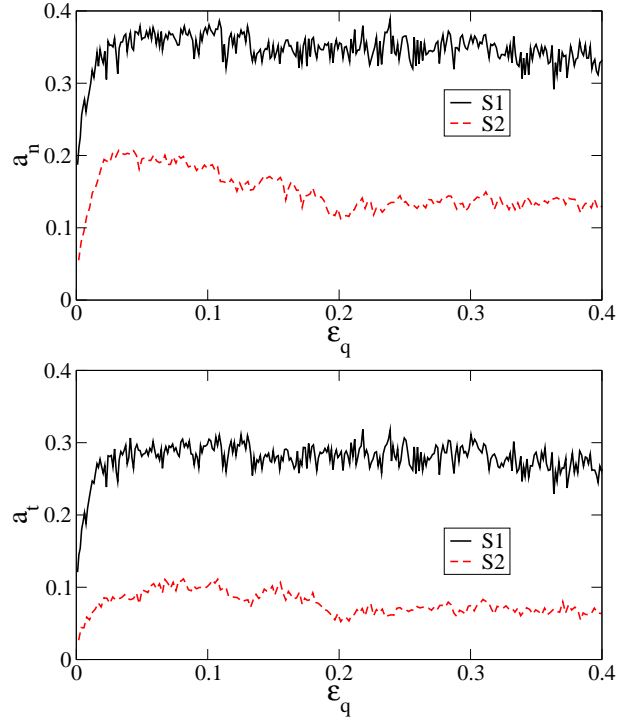


Figure 8: Evolution of force anisotropies a_n (a) and a_t (b) as a function of cumulative shear strain ϵ_q in samples S1 and S2.

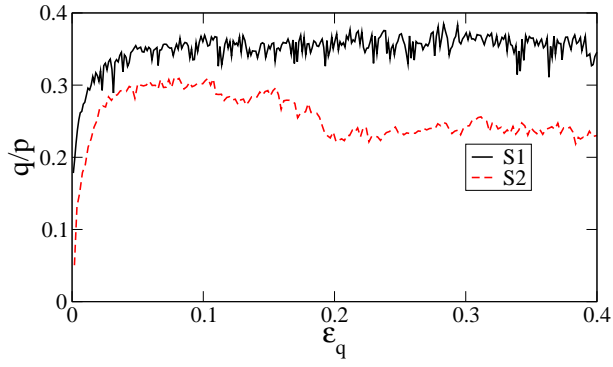


Figure 9: Normalized shear stress q/p as a function of cumulative shear strain for the samples S1 and S2.

comes from force anisotropy. The fabric anisotropy is generally low and partially inhibited by the presence of adhesion. Note also that adhesion between particles involves a force scale so that its contribution to the shear strength is mainly expressed through the Coulomb cohesion c (equation (1)), but it can also influence the internal angle of friction φ_c through fabric anisotropy.

The size polydispersity is an important factor that affects space-filling properties of granular materials. In particular, for a broad size span, the small particles fill and stabilize the pores between larger particles. As a result, larger force anisotropies and thus shear strengths are expected for higher levels of size polydispersity. Large particles capture strong force chains whereas smaller particles are mostly at the center of weak forces [Voivret et al.(2008)]. The details of force transmission and force anisotropy depend, however, on the size distribution and not only on the span. An expected effect of polydispersity is to allow for higher values of z_{max} and thus enhanced shear strength as predicted by equation (10).

7 Conclusion

In this paper, we presented a brief account of physical mechanisms that underly the critical-state shear strength of granular materials. The short-comings of the picture of granular friction in direct analogy with solid friction was discussed. Recalling the expansion of the stress tensor in force and fabric anisotropies, a model was presented for the accessible geometrical states within a harmonic representation of the microstructure. This model, consistent with numerical simulations, relates the critical-state fabric anisotropy to two isotropic limit states corresponding to the lowest and highest contact densities of a granular packing. The force anisotropy was analyzed in the light of the bimodal character of force transmission. It was shown that the shear strength is mainly sustained by the strong force network so that force anisotropy is mainly related to the aptitude of a granular assembly to build up strong force chains. Finally, the effect of material parameters with respect to fabric and force anisotropies was discussed.

Acknowledgments. N. Estrada and A. Taboada are acknowledged for figure 2 as well as many useful discussions about granular friction. I present my special thanks to S. Roux for interesting and inspiring ideas he has shared with me about the plasticity of granular media and its microscopic origins.

References

- [Azéma et al.(2008)] E. Azéma, F. Radjai, and G. Saussine. Quasistatic rheology and force transmission in a packing of polyhedral particles. *Submitted.*, 2008.
- [Azéma et al.(2007)] E. Azéma, F. Radjai, R. Peyroux, and G. Saussine. Force transmission in a packing of pentagonal particles. *Phys. Rev. E*, 76 : 011301, Jul 2007.

- [Bagi(1999)] K. Bagi. Microstructural stress tensor of granular assemblies with volume forces. *Journal of applied mechanics-Transactions of the ASME*, 66 (4): 934–936, December 1999.
- [Bardet and Proubet(1992)] J. P. Bardet and J. Proubet. Shear-band analysis in idealized granular material. *J. Eng. Mech.*, 118: 397, 1992.
- [Cambou(1993)] B. Cambou. From global to local variables in granular materials. In C. Thornton, editor, *Powders and Grains 93*, pages 73–86, Amsterdam, 1993. A. A. Balkema.
- [Christoffersen et al.(1981)] J. Christoffersen, M. M. Mehrabadi, and S. Nemat-Nasser. A micromechanical description of granular material behavior. *J. Appl. Mech.*, 48: 339–344, 1981.
- [Coppersmith et al.(1996)] S. N. Coppersmith, C.-h. Liu, S. Majumdar, O. Narayan, and T. A. Witten. Model for force fluctuations in bead packs. *Phys. Rev. E*, 53 (5): 4673–4685, 1996.
- [Corriveau et al.(1997)] D. Corriveau, S. B. Savage, and L. Oger. Internal friction angles: characterization using biaxial test simulations. In N. A. Fleck and A. C. E. Cocks, editors, *IUTAM Symposium on Mechanics of Granular and Porous Materials*, pages 313–324. Kluwer Academic Publishers, 1997.
- [Darve and Laouafa(2000)] F. Darve, and F. Laouafa. Instabilities in granular materials and application to landslides. *Mechanics of Cohesive-frictional Materials*. *Mechanics of Cohesive-frictional Materials*, 5: 627–652, 2000.
- [Herrmann et al.(1995)] H. J. Herrmann, A.N.B. Poliakov, and H. J. Tillemans. Simulating shear bands in granular solids. In *Non Linear Phenomena in Materials Science III*, volume 42-43, pages 195–203, Zug, 1995. Scitec Publ.
- [Majmudar and Behringer(2005)] T. S. Majmudar and R. P. Behringer. Contact force measurements and stress-induced anisotropy in granular materials. *Nature*, 435: 1079–1082, 2005.
- [Metzger(2004)] P. T. Metzger. Granular contact force density of states and entropy in a modified edwards ensemble. *Phys. Rev. E*, 70 : 051303, Nov 2004.
- [Mitchell and Soga(2005)] J. K. Mitchell and K. Soga. *Fundamentals of Soil Behavior, third edition*. Wiley, 2005.
- [Moreau(1997)] J. J. Moreau. Numerical investigation of shear zones in granular materials. In D. E. Wolf and P. Grassberger, editors, *Friction, Arching, Contact Dynamics*, pages 233–247, Singapore, 1997. World Scientific.
- [Mueth et al.(1998)] D. M. Mueth, H. M. Jaeger, and S. R. Nagel. Force distribution in a granular medium. *Phys. Rev. E*, 57: 3164, 1998.

- [Nedderman(1992)] R. M. Nedderman. *Statics and kinematics of granular materials*. Cambr. Univ. Press, Cambridge, 1992.
- [Nicot and Darve(2006)] F. Nicot and F. Darve. Micro-mechanical investigation of material instability in granular assemblies. *Int. J. of Solids and Structures*, 43: 3569-3595, 2006.
- [Oudafel and Rothenburg(2001)] H. Oudafel and L. Rothenburg. Stress-force-fabric relationship for assemblies of ellipsoids. *Mechanics of Materials*, 33 (4): 201–221, 2001.
- [Radjai et al.(1996)] F. Radjai, M. Jean, J. J. Moreau, and S. Roux. Force distribution in dense two-dimensional granular systems. *Phys. Rev. Lett.*, 77 (2): 274, 1996.
- [Radjai et al.(1998)] F. Radjai, D. E. Wolf, M. Jean, and J.J. Moreau. Bimodal character of stress transmission in granular packings. *Phys. Rev. Letter*, 80: 61–64, 1998.
- [Radjai et al.(2001)] F. Radjai, I. Preechawuttipong, and R. Peyroux. Cohesive granular texture. In P.A. Vermeer, S. Diebels, W. Ehlers, H.J. Herrmann, S. Luding, and E. Ramm, editors, *Continuous and discontinuous modelling of cohesive frictional materials*, pages 148–159, Berlin, 2001. Springer Verlag.
- [Radjai et al.(2004)] F. Radjai, H. Troadec, and S. Roux. Key features of granular plasticity. In S.J. Antony, W. Hoyle, and Y. Ding, editors, *Granular Materials: Fundamentals and Applications*, pages 157–184, Cambridge, 2004. RS.C.
- [Radjai et al.(1999)] F. Radjai, S. Roux, and J. J. Moreau. Contact forces in a granular packing. *Chaos*, 9 (3): 544–550, Sep 1999.
- [Rothenburg and Bathurst(1989)] L. Rothenburg and R. J. Bathurst. Analytical study of induced anisotropy in idealized granular materials. *Geotechnique*, 39: 601–614, 1989.
- [Rothenburg and Selvadurai(1981)] L. Rothenburg and A. P. S. Selvadurai. A micromechanical definition of the cauchy stress tensor for particulate media. In A. P. S. Selvadurai, editor, *Mechanics of Structured Media*, pages 469–486. Elsevier, 1981.
- [Roux and Radjai(2001)] S. Roux and F. Radjai. Statistical approach to the mechanical behavior of granular media. In H. Aref and J.W. Philips, editors, *Mechanics for a New Millennium*, pages 181–196, Netherlands, 2001. Kluwer Acad. Pub.
- [Staron et al.(2002)] L. Staron, J.-P. Vilotte, and F. Radjai. Preavalanche instabilities in a granular pile. *Phys. Rev. Lett.*, 89: 204302, 2002.
- [Staron et al.(2005)] L. Staron, F. Radjai, and J-P. Vilotte. Multi-scale analysis of the stress state in a granular slope in transition to failure. *Eur Phys J E Soft Matter*, 18 (3): 311–320, Nov 2005.

- [Staron and Radjai(2005)] L. Staron and F. Radjai. Friction versus texture at the approach of a granular avalanche. *Phys Rev E*, 72 : 041308, Oct 2005.
- [Taboada et al.(2006)] A. Taboada, N. Estrada, and F. Radjai. Additive decomposition of shear strength in cohesive granular media from grain-scale interactions. *Phys. Rev. Lett.*, 97 (9): 098302, Sep 2006.
- [Troadec et al.(2002)] H. Troadec, F. Radjai, S. Roux, and J.-C. Charmet. Model for granular texture with steric exclusions. *Phys. Rev. E*, 66: 041305, 2002.
- [Tsoungui et al.(1998)] O. Tsoungui, D. Vallet, and J.-C. Charmet. Use of contact area trace to study the force distributions inside 2d granular systems. *Granular Matter*, 1 (2): 65–69, 1998.
- [Vardoulakis and Sulem(1995)] I. Vardoulakis and J. Sulem. *Bifurcation analysis in geomechanics*. Chapman & Hall, London, 1995.
- [Vermeer(1990)] P. A. Vermeer. The orientation of shear bands in biaxial tests. *Géotechnique*, 40: 223, 1990.
- [Voivret et al.(2008)] C. Voivret, F. Radjai, J.-Y. Delenne, and M.S. El Youssoufi. Force transmission in polydisperse granular media. *submitted*, 2008.
- [Wood(1990)] D.M. Wood. *Soil behaviour and critical state soil mechanics*. Cambridge University Press, Cambridge, England, 1990.